RESEARCH ARTICLE

Shi-Xia Yu[1], Lv-Wen Zhou[2], Li-Qin Hu[1], Yu-Tong Jiang[1], Yan-Jie Zhang[1], Shi-Liang Feng[2], Yuling Jiao[3,4], Lin Xu[4,5] and Wen-Hui Lin[1,*]

ABSTRACT

[illegible abstract text]

KEY WORDS: Ovule initiation, Asynchrony, Auxin, Brassinosteroid

INTRODUCTION

The formation of lateral organ primordia is a significant event in the growth and development of plants and animals. Plants initiate lateral organ primordia continuously and at regular positions from the growing tip; these processes are strictly regulated by plant hormones and other(t)1INTR&3(r)17(as)51.(r)17y(t)1INTRr8(Au.2(pont)-214.5(al)ornts)iprimrm al

Bencivenga et al., 2012). The mutant of DELLA protein, a negative regulator of GA signaling, produces fruits with fewer seeds than those in wild type, indicating that loss of GA regulates ovule number (Gomez et al., 2018; Barro-Trastoy et al., 2020).

Auxin has been demonstrated to control primordia initiation in lateral root and shoot apical meristem (SAM) (Laskowski et al., 1995; Reinhardt et al., 2000). The combined action of differentially expressed and localized PIN1 proteins results in the formation of an auxin gradient, which mediates proper lateral root development (Casimiro et al., 2001; Benková et al., 2003). PIN1 polarity also causes changes in auxin levels to direct primordium development in the SAM (Heisler et al., 2005). In addition, the crosstalk between auxin and CK is essential for cell-type specification in the root, SAM and gynoecium. PIN1-GFP is expressed in the placenta and the epidermis cells of the ovule, and the DR5-GFP signal is visible after ovule protrusion (Galbiati et al., 2013). CUP-SHAPED COTYLEDON1 (CUC1) and CUC2 establish the boundaries of ovule primordia and control PIN1 expression in ovules (Galbiati et al., 2013; Gonçalves et al., 2015). Auxin triggers the expression of ANT and MONOPTEROS (MP), which are also required for ANT, CUC1 and CUC2 expression (Galbiati et al., 2013; Cucinotta et al., 2020). However, there is no detailed hypothesized model connecting PIN1 polarity, auxin maxima and whole ovule population initiation.

Overall, only a few studies focus on the earliest stage of ovule development. The detailed process of ovule primordia initiation remains unclear. Here, we report that ovules develop asynchronously in the same placenta, and ovule primordia initiate in different groups. Our results further show how PIN1 polarity and auxin gradient maxima in the placenta lead to the initiation of different groups of ovule primordia. We also establish a computational model describing the process of asynchronous ovule primordia initiation. BR signal promotes ovule number not only through increasing placenta length but also through stimulating ovule primordia initiation by strengthening auxin response. We also performed a microarray assay of the stage-specific gynoecium (removing the stigma and junction site of floral organs). Our comprehensive analysis revealed genes that functioned in ovule development. In conclusion, our results shed light on the detailed process of ovule primordia initiation and show how hormones integrate ovule primordia initiation and ovule development.

RESULTS
Ovule primordia initiate asynchronously on identical placentas
The protrusions, i.e. ovule primordia, are initiated by periclinal divisions of the subepidermal cells of the placenta at stage 9 (Bowman et al., 1991; Robinson-Beers et al., 1992). After a series of divisions, the ovule primordia differentiate and elongate along with the proximal-distal axis at stage 10 (Bowman et al., 1991; Robinson-Beers et al., 1992; Schneitz et al., 1995). Ovule development starts from stage 9, but the ovule shape differs between the beginning and end of stage 9, because stage 9 is relatively long. For easy observation and accurate description, we subdivided floral stage 9 into three substages: stages 9a, 9b and 9c, corresponding to the early, middle and late stage 9. If we consider the ovule primordium as a cylinder protruding from the placenta, there are at least three different shapes of ovule primordia at stage 9 based on the height and basal diameter of the cylinder. In the small/young ovule primordia (i.e. named O1 for convenience), the basal diameter of the ovule primordium is much larger than its height (Fig. S1A). In the middle age ovule primordia (O2), the basal diameter equals its height (Fig. S1B). In the large/old ovule primordia (O3), the basal diameter is much less than its height

(Fig. S1C). O1, O2 and O3 ovule primordia are small-bump shaped, dome shaped and O3 finger shaped, respectively.

At stage 8, there are no protrusions on the placenta (Fig. 1A,F). At stage 9a, four to six ovule primordia initiate on each placenta, and all ovule primordia are small-bump shaped (O1) (Fig. 1B,G). At stage 9b, there are seven to nine ovule primordia on each placenta and old ovule primordia that initiated at stage 9a are dome shaped (O2), while the young ovule primordia are small-bump shaped (O1) (Fig. 1C,H). The number of ovule primordia peaks at ten to 14 at stage 9c, and the oldest batch of ovule primordia is finger shaped (O3), the younger batch is dome shaped (O2) and the youngest batch is small-bump shaped (O1) (Fig. 1D,I). At stage 10, all ovules are finger shaped (O3), and the number and shape of ovules at each placenta show only minor differences (Fig. 1E,J). The quantitative analysis demonstrated that ovule primordia were all in O1 condition at stage 9a, and the ratio of O1 reduced at stage 9b-9c, suggesting the ovule initiated at stage 9a, and grew to O2 or O3 when the new young ovule (O1 condition) protruded (Fig. 1K). Finally, all ovules grew to O2 and O3 conditions, and the young ovule primordia (O1) initiation stopped gradually, with O1 ovule absent by stage 10 (Fig. 1K). There are different ages and shapes of ovules in each placenta, which illustrates that ovule primordia initiation is asynchronous.

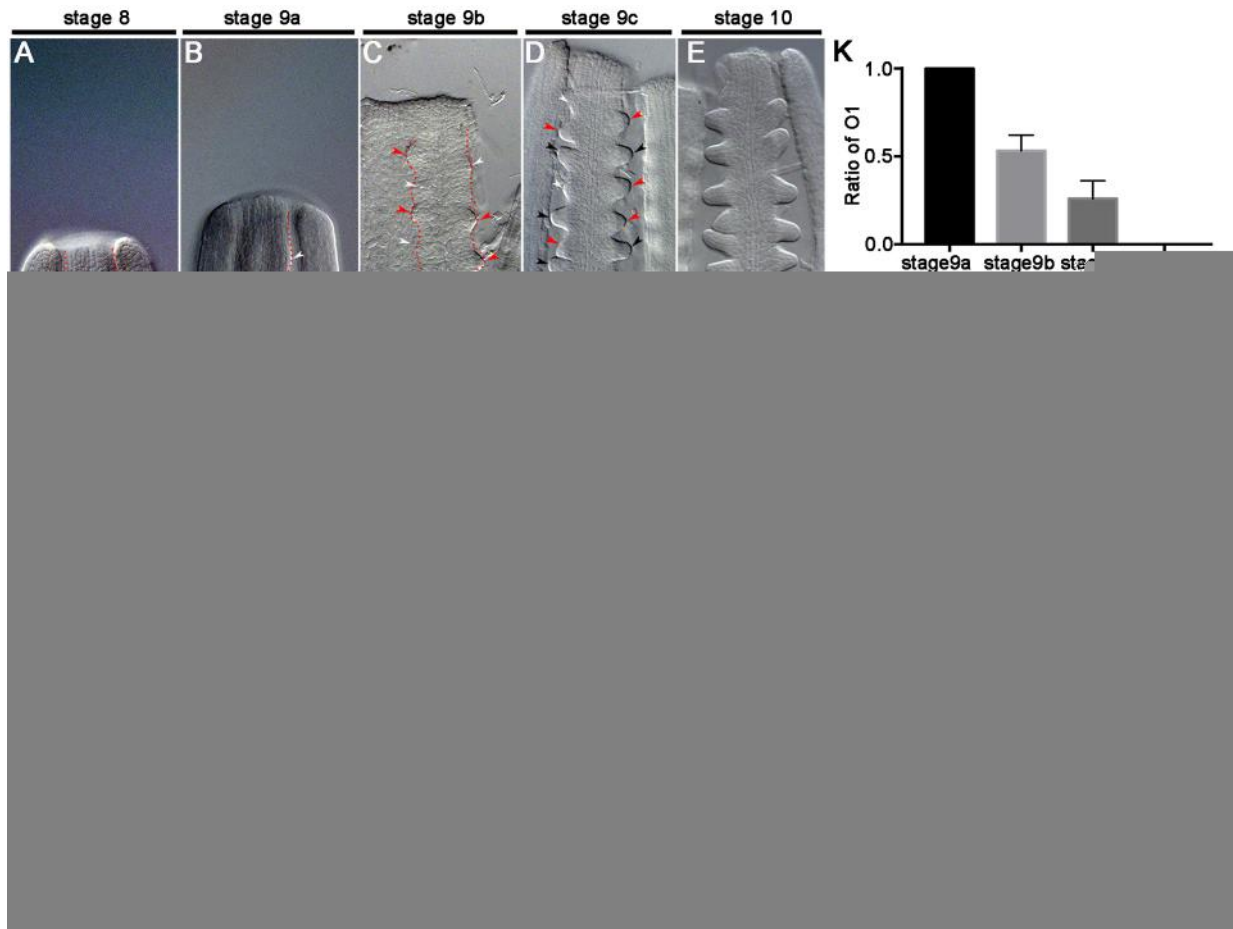### Ovule primordia initiate in different groups
For determining the initiation order of different ovule primordia, we observed the protrusion process in many placentae. Photographic analyses showed that the larger and smaller (O2 and O1 or O3 and O2) ovules arranged alternately in the placenta (Fig. 1C,D,H,I,L,M; Fig. S1D-F). But there was not always one smaller ovule between every two larger ovules because there was sometimes insufficient space for new ovule primordia between each two larger ovules (Fig. 1L,M; Fig. S1D-F). Generally, each ovule primordium has a different size and shape from that of its neighbors.

Although the ovule primordia initiate from the placenta in groups, ovule primordia belonging to the same group do not appear identical in size and shape (Fig. 1B,G). We decided to observe the largest ovule primordium out of six ovule primordia in every placenta at stage 9a, as this must be the ovule that initiates first in the placenta (assuming all ovules grow at a similar speed) (Fig. S1D). Observing this first ovule primordium is difficult because it initiates over a very short period of time. For easy statistics, we divided the placenta into the upper, middle and lower parts. We found that 45.5% of first protrusions appeared in the lower part, about 47.6% in the middle part and about 6.9% in the top part (Fig. S1G). These results suggest that the first ovule primordia initiate mainly from the middle and lower parts of the placenta.

CUC3, PIN1 and R2D2 signals indicate asynchronous initiation of ovule primordia
To confirm the asynchronous initiation of ovule primordia, we observed the expression of *ProCUC3::CFP* (Gonçalves et al., 2015) to show the boundaries between ovules and to indicate the number of ovule primordia forming at stage 9. When the ovule primordia forms at stage 9a, *ProCUC3::CFP* is expressed in the boundaries between each two ovule primordia; there are only a few boundaries formed, demonstrating that only four to seven ovules form at stage 9a (Fig. 2A,B). When more ovule primordia are formed at stage 9b, the clusters of *ProCUC3::CFP* signals are not evenly arranged, demonstrating that ovules are in different sizes (Fig. 2C,D).

It has been reported that PIN1 is expressed in ovule primordia (Benková et al., 2003; Galbiati et al., 2013). We observed the *ProPIN1:: PIN1-GFP* signal during the ovule initiation process. At stage 9a, the PIN1-GFP signal clustered to the ovule protrusions and there were only

Fig. 1. Ovule primordia initiation process in *Arabidopsis* placentae.

a few signal clusters detected in the placenta (Fig. 2E,F). At stage 9b, there were different ranges and intensities of PIN1-GFP expression in different cell clusters (Fig. 2G,H), demonstrating that there are ovules of different sizes in the same placenta.

R2D2 combines with DII-n3×Venus and mDII-ntdTomato to show auxin gradients in which the absence of DII fluorescence marks auxin accumulation (Brunoud et al., 2012; Liao et al., 2015). We also observed the *R2D2* expression pattern. At stage 9a, there are four to seven regions on the placenta where no signal is detected, these regions represent the position of the ovule primordia (Fig. 2I-K). At stage 9b, there are more regions with no signal, and the signal intensity is not even, which means that more ovule primordia initiate and the ovules are not the same size (Fig. 2L-N).

Based on the *CUC3*, *PIN1* and *R2D2* expression regions, we demonstrate that there are only a few ovule primordia initiating at stage 9a and that other ovules initiate later. These data indicate that the ovule initiation is asynchronous in the same placenta.

Ovule primordia develop asynchronously at subsequent stages

We examined the expression pattern of different markers to indicate the stage of ovules in the same placenta after ovule primorida initiation. *WUSCHEL* (*WUS*) mRNA is expressed in the ovule at stage

9-10 (Groß-Hardt et al., 2002). We used the *ProWUS::3xVENUS-N7* transgene to observe the ovule primordia formation (Zhang et al., 2017). *WUS* was not expressed before stage 9b (Fig. 3A,B), but was expressed from stage 9c, and its expression level increased with ovule primordia elongation (Fig. 3C-F). The intensity and distribution of *WUS* mRNA differs among ovules in the same placenta (Fig. 3G,H), suggesting that asynchronous development of ovules continues at stage 9c-10.

KNUCKLES (KNU) is expressed in the MMC throughout meiosis (Payne et al., 2004; Zhao et al., 2018). At stage 10, the stage of MMC specification, the *ProKNU::KNU-VENUS* signal exhibit three patterns: no signal, weak signal and strong signal (Fig. 3I,J). All three levels of KNU-VENUS signal were observed in the same placenta (Fig. S2A). At stage 11, we also observed different patterns of KNU localization: one nucleus in MMCs and two to four nuclei in megaspore cells during meiosis in the same placenta (Fig. 3K,L; Fig. S2B). These results indicate that ovule development remains asynchronous at the MMC differentiation and meiosis stages.

Next, we observed the expression pattern of *FM1*, a marker gene of the functional megaspore (FM) (Huanca-Mamani et al., 2005). We found that the *ProFM1::GUS* transgene was expressed in some ovules at stages of FM specification and division (stage 12a-12b)

(Fig. 3M). There are ovules with or without *ProFM1::GUS* signal in the same placenta (Fig. S2C), indicating that ovule development is still asynchronous at the FM specification stage.

Finally, we observed embryo sac (ES) development at stage 12 in the same placenta using optical sections with confocal laser

inflorescence apex with different concentrations of NPA and found that ovule primordia initiation was more sensitive than gynoecium development to NPA (Fig. S4).

Under mock control treatment, ovule primordia initiate normally (Fig. 5A,B,E,F; Fig. S4A,B): PIN1 levels increase in placentae, PIN1 polarity points towards the primordia tip (Fig. 5I,J,Q,R) and DR5 response maxima form at the primordia tips during the initiation (Fig. 5M,N,U,V). In the NPA-treated samples, although the gynoecium development is normal, the initiation of new ovule primordia stops, the existing ovule primordia keep growing at low NPA concentrations but the ovule growth finally arrests in high concentrations of NPA (Fig. 5C,D,G,H; Fig. S4C-H). PIN1 expression dramatically decreases and PIN1 polarity disappears at stage 9a-9b under NPA treatment (Fig. 5K,L,S,T). An auxin response maximum still forms in primordia tips but the intensity is decreased (Fig. 5O,P,W,X). These findings highlight that normal PIN1 polar localization and auxin response are essential for young ovule primordia initiation, and also demonstrate that ovule primordia are initiated in different groups.

Computational models predict asynchronous ovule primordia initiation

We developed a computational model to predict ovule primordia initiation regulated by dynamic PIN1 localization and auxin distribution. The model simplified placenta elongation, auxin distribution and ovule primordia initiation into a one-dimensional line to simulate a perfect state (Fig. 6A,B). In the model, auxin was transported between neighboring cells by PIN1, while PIN1 polarization was determined by the auxin concentration in neighboring cells (Fig. 6C). Auxin was distributed almost evenly with tiny perturbations before initiation. Placenta cells expanded and divided to simulate placenta elongation (Fig. 6B). To smooth the spatial variation in auxin concentration, we performed a cubic spline interpolation on the simulation results. We showed the spatiotemporal distribution of auxin after interpolation and the length of the placenta (Fig. 6D). The simulation results showed that, in response to the action of PIN, the initial uniform distribution of auxin spontaneously changes to produce several localized maxima, which induce the auxin response and the initiation of the first group of ovule primordia
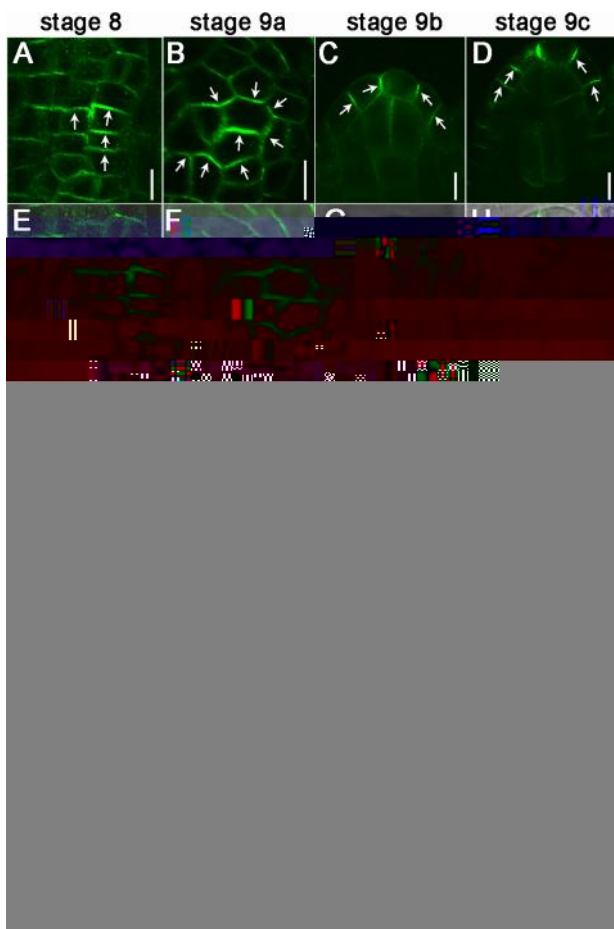
Fig. 4. Dynamic distribution of PIN1 and auxin in the process of ovule primordia initiation.
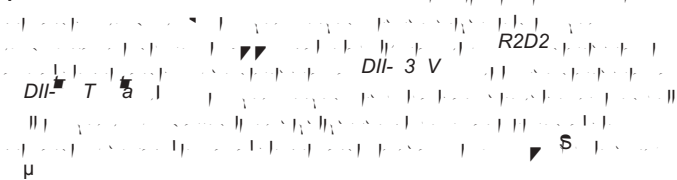
(Fig. 6D; Movie 1). As the cells expand and divide, the placenta elongates (Fig. 6D; Movie 1). Subsequently, a second group of auxin maxima is formed, which induces the auxin response and the initiation of the second group of ovule primordia (Fig. 6D; Movie 1). Given the model assumptions, these results suggest that new ovule primordia initiation requires PIN1 polarity and the formation of localized auxin maxima, and that ovule primordia initiate in different groups tightly accompanied by the auxin response.

BR promotes ovule primordia initiation

Our previous research illustrated that BR influences ovule number through transcriptional regulation of the early ovule development-related genes *ANT*, *HLL* and *AP2* (Huang et al., 2013). To explore whether BR affects ovule initiation, we observed ovule primordia initiation in the BR-insensitive mutant *bin2-1* and the BR-enhanced mutant *bzr1-1D* (Li and Nam, 2002; Wang et al., 2002). At stage 8, no protrusions appear in the placentae of wild type, *bin2-1* and *bzr1-1D* (Fig. 7A,D,G). At stage 9a, the placental length is ~180 µm in Col-0 when the first batch of ovule primordia initiate (Fig. 7B,J,L). At the same developmental stage, *bin2-1* and *bzr1-1D* have smaller and larger placentae, respectively (Fig. 7E,H,J,L). In addition, there is a

lower and a higher number of ovule primordia in the first group in *bin2-1* and *bzr1-1D*, respectively (Fig. 7B,E,H,K). These results suggest that BR contributes to placenta elongation and the protrusion of the ovules of the first batch. Similar results were observed at stage 9c (Fig. 7C,F,I-K). The phenotype of the crowded ovule in *bzr1-1D* at stage 9 indicates higher ovule density (the ratio of the ovule number to the placenta length) (Fig. S5) (Jiang et al., 2020), and suggests that BR increases seed number not only through promoting placentae elongation but also through promoting ovule primordia initiation. Flowers treated with 2,4-epibrassinolide (eBL) at stage 8-9 exhibited increased DR5 signal, indicating a significantly enhanced auxin response (Fig. 7M-U). This result demonstrates that BR also affects the auxin response to promote ovule primordia initiation.

Transcriptomic analysis of gene expression during ovule development

To obtain the global gene expression trends during ovule development, we collect samples of the gynoecium in developmental stages 9-10, 11 and 12 to perform a microarray assay. 4694 genes are identified as differentially expressed genes (DEGs) from 19,665 genes (fold change≥2.0 and $P≤0.05$) (Figs S6A and S7A,B; Table S1). Hierarchical clustering of the DEGs reveal there are relatively similar transcription patterns at stage 9-10 and stage 11, but different expression patterns are found at stage 12 compared with those at stages 9-11 (Fig. S6B). In addition, the enriched Kyoto Encyclopedia of Genes and Genomes (KEGG) pathways and Gene Ontology (GO) analysis indicate that vigorous hormone signaling and biosynthetic/metabolic processes are required during ovule development (Fig. S7C,D).

To explore the possible functions of the DEGs in ovule development, clustering analysis by STEM is used to further divide the DEGs into 12 clusters of clear and distinct expression profiles. The top six clusters are exhibited in Fig. S6C. Clusters 2, 3 and 6 contain genes highly expressed at stage 9-10, suggesting that these genes function during ovule initiation and development. Genes reported to influence these processes, such as *CUC*, *ANT*, *KNU* and *WUS*, are identified in DEGs, and their transcription patterns are consistent with the expression pattern of our marker lines or previous reports (Figs 2 and 3; Table S1) (Schneitz et al., 1998; Groß-Hardt et al., 2002; Payne et al., 2004; Gonçalves et al., 2015).

Our results also illustrated some regulators of shoot apical meristem (SAM) development and maintenance, such as *SHOOT MERISTEMLESS* (*STM*), *ASYMETRIC LEAVES 2* (*AS2*), *KNOTTED-LIKE FROM ARABIDOPSIS THALIANA2* (*KNAT2*) (Barton and Poethig, 1993; Lincoln et al., 1994; Semiarti et al., 2001). We also identified *WOX1*, *WOX12* and *WOX13* at stage 9-10, suggesting that these WOX genes play essential roles in ovule primordia formation (Table S1). The WOX gene family has been reported to regulate embryogenesis, stem cell homeostasis and organ formation (Laux et al., 1996; Haecker et al., 2004; Deveaux et al., 2008), suggesting that they are reasonable players in ovule initiation and development. Clusters 1, 4 and 5 contained genes highly expressed at stage 12, indicating that they play an important role in embryo sac development and ovule micropyle formation. For example, unfertilized embryo sac mutant (UNE), which exhibits defects in fertilization (Pagnussat, 2005), was identified in cluster 4 (Table S1). In addition to already identified genes, our DEGs also included homologs of known genes and completely new genes. Rapid alkalinization factor (RALF) family members, e.g. small peptide RALF4/19/34, play an important role during gametogenesis and fertilization (Haruta et al., 2014; Ge et al., 2017). We found that many other RALF family members were highly expressed at stage 12,
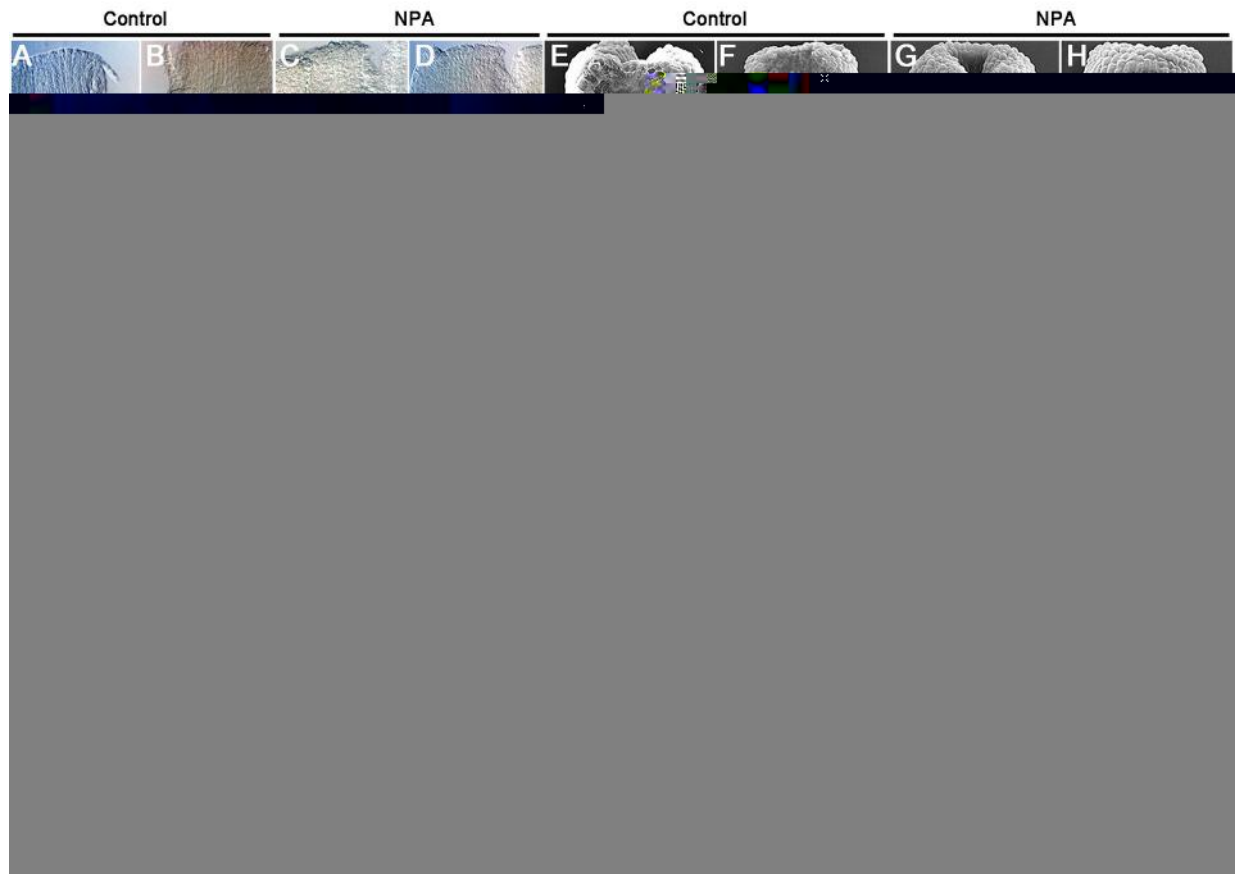
Fig. 5. NPA treatment inhibits the initiation of new ovule primordia via its effects on PIN1 localization and auxin response.

suggesting these RALF peptides also participate in male-female interaction. Receptor-like kinases (RLKs), including POLLEN-SPECIFIC RECEPTOR-LIKE KINASE, ANXUR, MALE DISCOVERER and others, play essential roles in male-female communication (Takeuchi and Higashiyama, 2016; Wang et al., 2016; Ge et al., 2017). Other RLKs are highly expressed at stage 12, such as RLP31, MRH1 and FLS2, suggesting that these RLKs also function in male-female communication. Some DEGs have not been reported previously (Table S1) and other DEGs are currently uncharacterized (e.g. *MYB*, *WRKY*, *CYP*, etc.) but with limited clues, indicating new candidates and regulatory mechanisms for ovule development that are worthy of future investigation.

Plant hormones have been reported to play roles in gynoecium development, especially auxin, BR, CK and GA (Colombo et al., 2008; Reyes-Olalde et al., 2013; Zúñiga-Mayo et al., 2019; Cucinotta et al., 2020). Among the DEGs, we identified lots of hormone-related genes, including important components of their biosynthesis, transport and response, indicating the hormonal regulation in ovule development (Table S2). Hierarchical clustering of 39 auxin-related genes shows that most of the genes encoding AUX/IAA proteins were upregulated, and auxin response factors (ARFs) and auxin metabolic genes were downregulated (Fig. S6D; Table S2). The expression patterns of auxin biosynthesis genes and auxin polar transporters were different from stage 9 to stage 12, which implied that these genes functioned at different stages and took part in

different events. For example, PIN1 was expressed at stage 9-10, which mainly coincides with ovule initiation, consistent with the *ProPIN1::PIN1-GFP* expression pattern (Fig. 2E–H; Fig. S6D; Table S2). Among the 21 BR-related genes, most BR synthesis genes were gradually downregulated, while BR response genes were mostly upregulated (Fig. S6E; Table S2), indicating that BR signaling remains active during ovule development and that the BR biosynthesis is feedback inhibited. Hierarchical clustering of 23 CK-related genes showed that the expression patterns of CK synthase, glucosyltransferase, CK receptors and CK response genes were gradually downregulated, and CK hydrolase and transport enzyme gene were upregulated, indicating that CK played essential roles in early ovule development and would be downregulated in late ovule development (Fig. S6F; Table S2). For GA-related genes, GA biosynthetic and response genes were highly expressed at stage 12-13, but genes in the GA signaling pathway were highly expressed at stage 9-10 (Fig. S6G; Table S2). Above all, hormone signaling is active throughout ovule development; each hormone is accurately modulated to regulate ovule development.

DISCUSSION
Asynchronous ovule primordia initiation is important for plant reproductive development
Previous studies have mentioned ovule primordia formation (Bartrina et al., 2011; Huang et al., 2013; Gonçalves et al., 2015)

Fig. 6. Schematic diagram of the model and its principle.

and ovule development, such as the nucellus identity, integument initiation and embryo sac development (Villanueva et al., 1999; Erbasol Serbes et al., 2019). Here, we have observed the detailed process of ovule primordia initiation by DIC and SEM (Fig. 1). Our results show that ovule primordia initiate asynchronously in the same placenta, and that new ovule primordia initiate mainly between older neighboring ovule primordia (Fig. 8). The first batch of ovule primordia appears at stage 9a (Fig. 8C). Later, two groups of ovule primordia exist on the same placenta, and can easily be distinguished according to their size and shape (Fig. 8E). Statistical analysis demonstrated that ovules on the same placenta are mainly at two continuous developmental stages. The third batch of ovule primordia initiated normally at the bottom and top of the placenta, and differed significantly from the size and shape of the first two groups. Our hypothesis illustrates that the ovule population initiation is an interrelated process. Until now, published models mainly described single ovule primordium initiation and the signals between the primordium and its two boundaries (Galbiati et al., 2013; Cucinotta et al., 2020). Our hypothesis describes the relationship of neighboring ovule primordia during the initiation.

The close relationship between larger placental size and enhanced seed number in some mutants (*ckx3 ckx5* and *bzr1-1D*) indicates that placenta size is one factor that affects ovule primordia initiation (Bartrina et al., 2011). However, the limited examples cannot clarify whether a larger placenta causes more primordia initiation in the

first and the second rounds, or whether there are more rounds of primordia initiation. Here, we demonstrate that the increased ovule number in the BR-signal-enhanced mutant comes from larger placental size and increased ovule primordia initiation in the first and second batches (Fig. 7). Microscopic analyses show that the larger and smaller ovules are not arranged evenly (Fig. 1C,D,H,I). This could be reasonably explained by the insufficient boundary of new ovules between some larger ovules. If the boundary is large enough, two young ovule primordia will initiate.

Ovule primordia continue to develop asynchronously at subsequent stages

Although previous studies indictaed that ovules at different stages (mainly 2-3) exist in the same gynoecium (Christensen et al., 1997), the reason remained unclear. Our results reveal there are different expression patterns of marker genes at different ovules in the same placenta, indicating that ovule primordia initiates mainly in two batches and grows out at a similar speed, leading to the ovules in the same gynoecium developing asynchronously from ovule primordia initiation (stage 9a) to embryo sac maturation (stage 12c) (Fig. 3). Previous reports have shown that pollen tubes preferentially guide to ovules at the middle pistil but not to the topper ovules (Feng et al., 2019). A reasonable explanation is that the pollen tube guiding sequence correlates with the ovule maturing sequence. The asynchronous initiation of ovule primordia is significant in plant reproductive development. The existing ovules can survive environmental stress but new ovules cannot grow out, which would be the effective way for the plant to allocate nutrition and control the number of offspring. Previous reports did not completely exclude the possibility that ovules initiated simultaneously but grew out at different speeds. Our results indicate the high possibility of asynchronous ovule initiation because only 5-7 ovules protrude firstly in one placenta, and more ovules of different sizes and shapes exist in the same placenta and at the same time at floral stage 9b-9c (Figs 1 and 2), and so on.

Transcriptomics analysis illustrates that the expression of hormone-related genes is accurately regulated during this process, indicating that those hormones maintain the normal developmental process of ovules (Fig. S6). Auxin is an important player in different processes of ovule development, indicating auxin functions in the whole process. BR signal is also activated during whole-ovule development, and BR promotes ovule initiation by enhancing placenta elongation and the auxin response (Fig. 7), as well as by transcriptional regulation of genes involved in early ovule development (Huang et al., 2013). CK promotes placenta activity to establish supernumerary ovules at early stages (Bartrina et al., 2011). GA inhibits ovule primoridia initiation. Transcriptomics analyses of the placenta were carried out in the previous studies (Skinner and Gasser, 2009; Matias-Hernandez et al., 2010); our systemic analysis of the whole developmental processes of ovules identified new candidate genes involved in ovule development. The DEGs identified by our transcriptomics analysis largely overlap with the DEGs listed by Skinner and Gasser (2009), indicating that our transcriptional analysis worked well. Compared with the genes expressed in placentae (identified by Matias-Hernandez et al., 2010), we identified 5086 new genes involved in ovule initiation in stage 9-10 (S1). Some of them are involved in pattern formation, such as ASYMMETRIC LEAVES2-LIKE1, FASCIATA1 (FAS1), FAS2, ULTRAPETALA2 and POLTERGEIST-LIKE1 (Kaya et al., 2001; Chalfun-Junior et al., 2005; Song et al., 2006; Monfared et al., 2013), indicating that they are involved in ovule primordia initiation and formation. In addition, the DEGs in ovule primordia initiation and in magasporogenesis/megagametogenesis are very different. The genes

Fig. 7. Ovule primordia initiation and auxin response in BR-related mutant at stage 8-9.
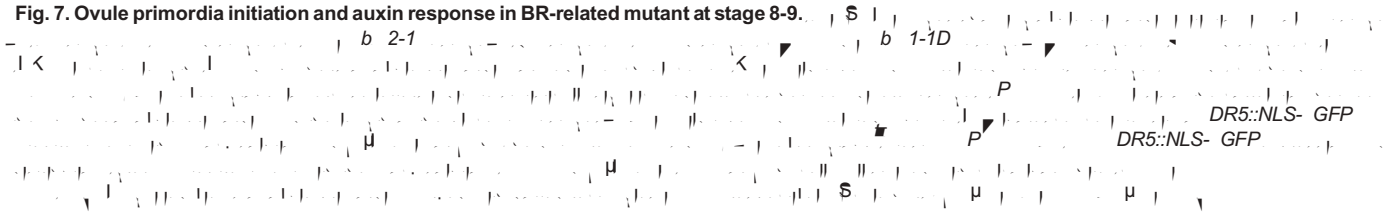
highly expressed in ovule primordia initiation have similar characteristics to meristem tissue, which is repressed in ovule development, suggesting that the genes regulating ovule initiation might be different from the genes regulating ovule development.

Homeostasis of PIN1 and auxin flow correlate asynchronous ovule primordia initiation

Unlike the process of lateral root primordia initiation from pericycle cells, ovule primordia initiate from the subepidermal layers by periclinal division (Vaughan, 1995). Previous research has reported that new primordium initiates between the old primordia in SAM (Heisler et al., 2005; Smith et al., 2006). After initiation of older primordia, new primordium is identified in the enlarged area between old primordia (Heisler et al., 2005). PIN1 expression gradually increases in new primordium and its neighboring cells, and PIN1 polarity points to the new primordium (Heisler et al., 2005). DR5 signal gradually appears at the top of the primordium (Heisler et al., 2005). After protrusion of the primordium, the expression of PIN1 decreases significantly, and the polarity of PIN1-GFP in epidermal cells at the base of the primordium reverses towards the center of meristem and adjacent areas (Heisler et al., 2005). DR5 signal continues to be expressed during the initiation process (Heisler et al., 2005).

Whereas the SAM is dome shaped, the placenta is the linear structure and the ovule primordia are distributed linearly among the placenta, whereas leaf and flower primordia are distributed among a

circle of the central zone of the SAM. Our results reveal the dynamic distribution of PIN1 in placenta. During ovule primordia initiation, PIN1 expression increases on the transverse and lateral sides in some placental cells, indicative of auxin flow to form localized maxima, thus triggering the initiation of the first group of ovule primordia (Fig. 8A,B,G). After the protrusions, PIN1 polar distribution travels towards to primordia tips; thus, auxin accumulates there (Fig. 8C,D,G). As the placenta grows, PIN1 polarity may be reversed in old primordia and new PIN1 polarity occurs in the placental cells between older primordia (i.e. boundaries), which consequently initiates new protrusions (Fig. 8E-G). The computational model mimics these processes (Fig. 6). New primordium is initiated within the elongated boundary between neighboring older primordia in the SAM and placenta, indicating that there is a conserved mechanism in ovule primordia initiation. When gynoecium is treated with NPA, PIN1 polar distribution is dramatically reduced and auxin response maxima still form in existing primordia tips but at a much lower level (Fig. 5). Importantly, there is no re-localization of PIN1 to the boundaries, which arrests new ovule primordia initiation, although the old primordia can keep growing (Fig. 5; Fig. S4).

Our results also illustrate that modified BR signals change the placenta size and ovule initiation. The decreased ovule density of *bin2-1* and the increased ovule density of *bzr1-1D* (Fig. 7J,L) indicate that BR not only promotes placenta elongation, but also stimulates ovule primordia initiation. Our previous work reported that BR positively regulated ovule number through transcriptional

DEVELOPMENT

regulation of early ovule development-related genes *ANT*, *HLL* and *AP2* (Schneitz et al., 1998; Huang et al., 2013). Here, we have found another way for BR to promote ovule initiation: by strengthening auxin response. The interaction of BR with auxin in root development has been well investigated (Hardtke, 2007; Cho et al., 2014; Oh et al., 2014; Tian et al., 2018; Sun et al., 2020), and our results reveal that the integration of BR and auxin promotes ovule development, indicating that the interaction of BR and auxin contributes to another developmental process.

In conclusion, our results show that ovule primordia initiate asynchronously. The accurate localization of PIN1, the formation of local auxin response maxima and elongation of the placenta are the main factors that determine this asynchrony initiation. Hormone signaling remains active and is modulated accurately to regulate ovule development.

MATERIALS AND METHODS

Plant material and growth conditions

Arabidopsis thaliana (Columbia-0) from ABRC (http://www.arabidopsis.org/) was used as wild-type or transgenic material, and plants used in this study include *bzr1-1D* (Wang et al., 2002), *bin2-1* (Li and Nam, 2002), *ProPIN1::PIN1-GFP* (Heisler et al., 2005), *ProWUS::3xVENUS-N7* (Zhang et al., 2017) and *ProKNU::KNU-VENUS* (Zhao et al., 2018), which have been described previously. Plants were grown in a 10:10:1 mix of peat substrate: vermiculite: perlite under a 16 h-light/8 h-dark photoperiod at 22±2°C. For growth on plates, surface-sterilized *Arabidopsis* seeds were placed on half-strength Murashige and Skoog (MS) basal medium. Plates were kept at 4°C for 3 days, then transferred to a growth chamber (Percival) with a 16 h-light/8 h-dark photoperiod at 22°C. The wild-type plants were transformed by the floral dip method using *Agrobacterium tumefaciens*

and

$$f_{i,j} = E_p(p_{i,j}a_i - p_{j,i}a_j), \tag{2}$$

where cell j is the neighbor of cell i, G_a is the degradation rate, A is related to the synthesis rate, D_a is the diffusion coefficient, E_p is the efficiency of the PIN1 efflux carrier, and $f_{i,j}(=f_{j,i})$ is the net flow of auxin by PIN1 from cell i to cell j, consisting of auxin efflux and influx. The first term of the right-hand side of Eqn 1 indicates that auxin is constantly synthesized and degraded at a constant rate; the second term indicates that auxin is transported by PIN1; the third term represents the diffusion of auxin between neighboring cells.

The change in PIN1 density ($p_{i,j}$) is described as follows:

$$\frac{dp}{}$$

References

Barro-Trastoy, D., Carrera, E., Baños, J., Palau-Rodríguez, J., Ruiz-Rivero, O., Tornero, P., Alonso, J. M., López-Díaz, I., Gómez, M. D. and Pérez-Amador, M. A. *Pa J.* **102**

Barton, M. K. and Poethig, R. S. *D* **119**

Bartrina, I., Otto, E., Strnad, M., Werner, T. and Schmülling, T. *A ab a a a Pa C* **23**

Bencivenga, S., Simonini, S., Benková, E. and Colombo, L. *A ab Pa C* **24**

Benková, E., Michniewicz, M., Sauer, M., Teichmann, T., Seifertová, D., Jürgens, G. and Friml, J. *C* **115**

Bowman, J. L., Smyth, D. R. and Meyerowitz, E. M. *A ab Pa C* **1**

Bowman, J. L., Drews, G. N. and Meyerowitz, E. M. *AGAMOUS Pa C* **3**

Brambilla, V., Battaglia, R., Colombo, M., Masiero, S., Bencivenga, S., Kater, M. M. and Colombo, L. *A ab Pa C* **19**

Brunoud, G., Wells, D. M., Oliva, M., Larrieu, A., Mirabet, V., Burrow, A. H., Beeckman, T., Kepinski, S., Traas, J., Bennett, M. J. et al. *Na* **482**

Casimiro, I., Marchant, A., Bhalerao, R. P., Beeckman, T., Dhooge, S., Swarup, R., Graham, N., Inzé, D., Sandberg, G. and Casero, P. J. *A ab Pa C* **13**

Chalfun-Junior, A., Franken, J., Mes, J. J., Marsch-Martinez, N., Pereira, A. and Angenent, G. C. *ASYMMETRIC LEAVES2-LIKE1 A ab Pa M . B* **57**

Cho, H., Ryu, H., Rho, S., Hill, K., Smith, S., Audenaert, D., Park, J., Han, S., Beeckman, T., Bennett, M. J. et al. *Na C B* **16**

Christensen, C. A., King, E. J., Jordan, J. R. and Drews, G. N. *A ab G S . Pa R* **10**

Colombo, L., Battaglia, R. and Kater, M. M. *A ab T Pa S* **13**

Cucinotta, M., Colombo, L. and Roig-Villanova, I. *F . Pa S* **5**

Cucinotta, M., Di Marzo, M., Guazzotti, A., de Folter, S., Kater, M. M. and Colombo, L. *J. E . B* **71**

Deveaux, Y., Toffano-Nioche, C., Claisse, G., Thareau, V., Morin, H., Laufs, P., Moreau, H., Kreis, M. and Lecharny, A. *BMC E . B* **8**

Elliott, R. C., Betzner, A. S., Huttner, E., Oakes, M. P., Tucker, W. Q. J., Gerentes, D. and Smyth, P. D. R. *Pa C* **8**

Erbasol Serbes, I., Palovaara, J. and Groß-Hardt, R. *C . T . D . B* **131**

Favaro, R., Pinyopich, A., Battaglia, R., Kooiker, M., Borghi, L., Ditta, G., Yanofsky, M. F., Kater, M. M. and Colombo, L. *Pa C* **15**

Feng, H., Liu, C., Fu, R., Zhang, M., Li, H., Shen, L., Wei, Q., Sun, X., Xu, L., Ni, B. et al. *M . Pa* **12**

Fujita, H. and Kawaguchi, M. *PL S C . B* **14**

Galbiati, F., Sinha Roy, D., Simonini, S., Cucinotta, M., Ceccato, L., Cuesta, C., Simaskova, M., Benkova, E., Kamiuchi, Y., Aida, M. et al. *Pa J.* **76**

Ge, Z., Bergonci, T., Zhao, Y., Zou, Y., Du, S., Liu, M.-C., Luo, X., Ruan, H., García-Valencia, L. E., Zhong, S. et al. *S* **358**

Gomez, M. D., Barro-Trastoy, D., Escoms, E., Saura-Sánchez, M., Sánchez, I., Briones-Moreno, A., Vera-Sirera, F., Carrera, E., Ripoll, J.-J., Yanofsky, M. F. et al. *D* **145**

Gonçalves, B., Hasson, A., Belcram, K., Cortizo, M., Morin, H., Nikovics, K., Vialette-Guiraud, A., Takeda, S., Aida, M., Laufs, P. et al. *CUP-SHAPED COTYLEDON Pa J.* **83**

Li, L., Xu, J., Xu, Z.-H. and Xue, H.-W. ... *Pa C* **17**

Li, B.-F., Yu, S.-X., Hu, L.-Q., Zhang, Y.-J., Zhai, N., Xu, L. and Lin, W.-H. ... *F . Pa S*. **9**

Liao, C.-Y., Smet, W., Brunoud, G., Yoshida, S., Vernoux, T. and Weijers, D. ... *Na . M* **12**

Lincoln, C., Long, J., Yamaguchi, J., Serikawa, K. and Hake, S. ... *Pa C* **6**

Marsch-Martínez, N. and de Folter, S. ... *C . O . Pa B*. **29**

Matias-Hernandez, L., Battaglia, R., Galbiati, F., Rubes, M., Eichenberger, C., Grossniklaus, U., Kater, M. M. and Colombo, L. ... *Pa C* **22**

Modrusan, Z., Reiser, L., Feldmann, K. A., Fischer, R. L. and Haughn, G. W. ... *Pa C* **6**

Monfared, M. M., Carles, C. C., Rossignol, P., Pires, H. R. and Fletcher, J. C. *ULT1 ULT2 ... M. a* **6**

Nemhauser, J. L., Feldman, L. J. and Zambryski, P. C. ... *ETTIN ... D* **127**

Nole-Wilson, S., Azhakanandam, S. and Franks, R. G. ... *AINTEGUMENTA REVOLUTA ... D . B*. **346**

Oh, E., Zhu, J.-Y., Bai, M.-Y., Arenhart, R. A., Sun, Y. and Wang, Z.-Y. ... *L* **3**

Pagnussat, G. C. ... *D* **132**

Payne, T., Johnson, S. D. and Koltunow, A. M. *KNUCKLES KNU ... D* **131**

Pinyopich, A., Ditta, G. S., Savidge, B., Liljegren, S. J., Baumann, E., Wisman, E. and Yanofsky, M. F. ... *Na* **424**

Reinhardt, D., Mandel, T. and Kuhlemeier, C. ... *T Pa C* **12**

Reiser, L., Modrusan, Z., Margossian, L., Samach, A., Ohad, N., Haughn, G. W. and Fischer, R. L. *BELL1 ... C* **83**

Reyes-Olalde, J. I., Zuñiga-Mayo, V. M., Chávez Montes, R. A., Marsch-Martínez, N. and de Folter, S. *T Pa S*. **18**

Robinson-Beers, K., Pruitt, R. E. and Gasser, C. S. ... *Pa C* **4**

Schneitz, K., Hulskamp, M. and Pruitt, R. E. ... *Pa J*. **7**

Schneitz, K., Baker, S. C., Gasser, C. S. and Redweik, A. ... *HUELLENLOS*

Semiarti, E., Ueno, Y., Tsukaya, H., Iwakawa, H., Machida, C. and Machida, Y. *AINTEGUMENTA ... D* **125**

Shi, D.-Q. and Yang, W.-C. ... *C . O . Pa B*. **14**

Skinner, D. J. and Gasser, C. S. *BMC Pa B*. **9**

Smith, R. S., Guyomarc'h, S., Mandel, T., Reinhardt, D., Kuhlemeier, C. and Prusinkiewicz, P. ... *USA* **103**

Smyth, D. R., Bowman, J. L. and Meyerowitz, E. M. ... *Pa C* **2**

Song, S.-K., Lee, M. M. and Clark, S. E. ... *D* **133**

Steeves, T. and Sussex, I. ... *Pa D*

Sun, L., Feraru, E., Feraru, M. I., Waidmann, S., Wang, W., Passaia, G., Wang, Z.-Y., Wabnik, K. and Kleine-Vehn, J. *B . 4*

Takeuchi, H. and Higashiyama, T. ... *Na* **531**

Theißen, G., Kim, J. T. and Saedler, H. ... *J. M . E*. **43**

Theißen, G. ... *C . O . Pa B*. **4**

Tian, H. Y., Lv, B. S., Ding, T. T., Bai, M. Y. and Ding, Z. J. ... *F . Pa S*. **8**

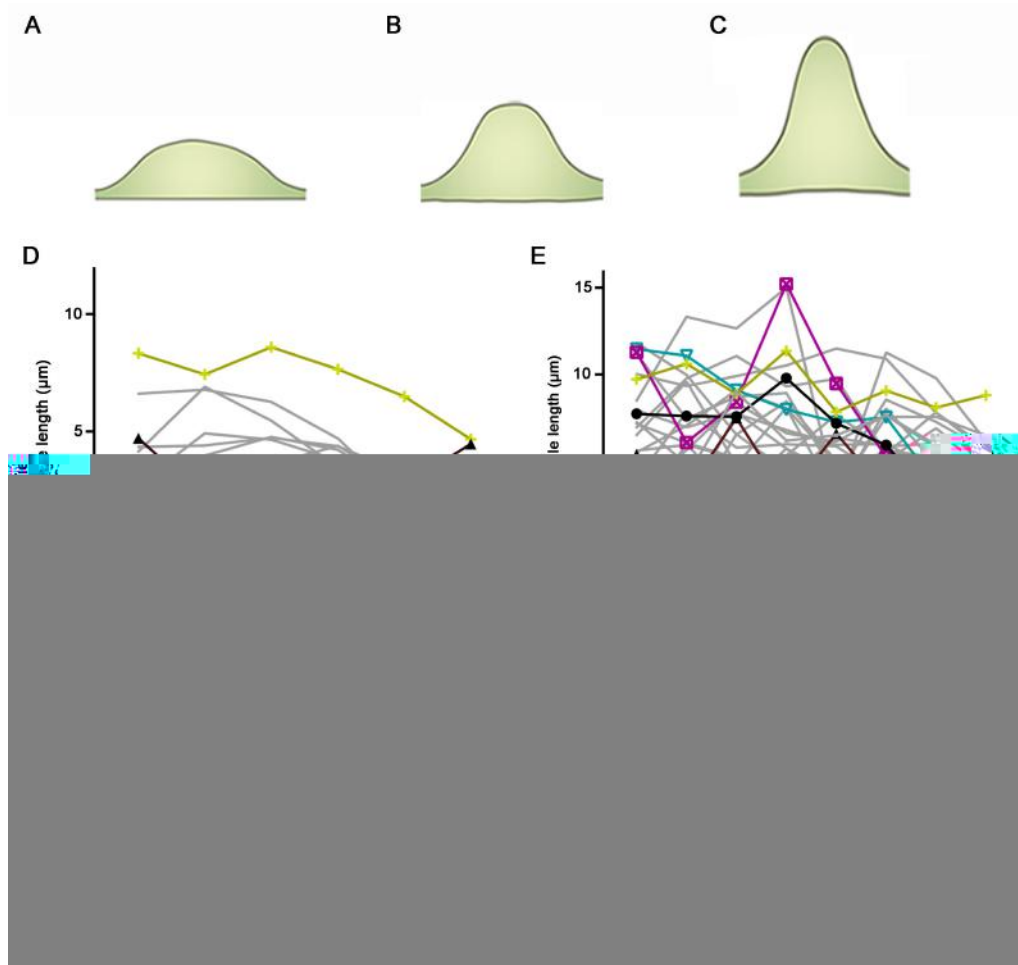Ursache, R., Andersen, T. G., Marhavý, P. and Geldner, N. ... *Pa J*. **93**

Vaughan, J. G. ... *Ca ab a- a ... B . J.L . S*. **55**

Villanueva, J. M., Broadhvest, J., Hauser, B. A., Meister, R. J., Schneitz, K. and Gasser, C. S. ... *G D* **13**

Wang, Z.-Y., Nakano, T., Gendron, J., He, J., Chen, M., Vafeados, D., Yang, Y., Fujioka, S., Yoshida, S., Asami, T. et al. ... *D . C* **2**

Wang, T., Liang, L., Xue, Y., Jia, P.-F., Chen, W., Zhang, M.-X., Wang, Y.-C., Li, H.-J. and Yang, W.-C. ... *Na* **531**

Zhang, T.-Q., Lian, H., Zhou, C.-M., Xu, L., Jiao, Y. and Wang, J.-W.

Figure S1. Quantification of ovule primordia height in different placentae at representative stages.

(A–C) The sketch of different ovule primordia shapes at stage 9 to stage 10: O1 shown small-bump-shaped (A), O2 shown dome-shaped (B), and O3 shown finger-shaped (C).

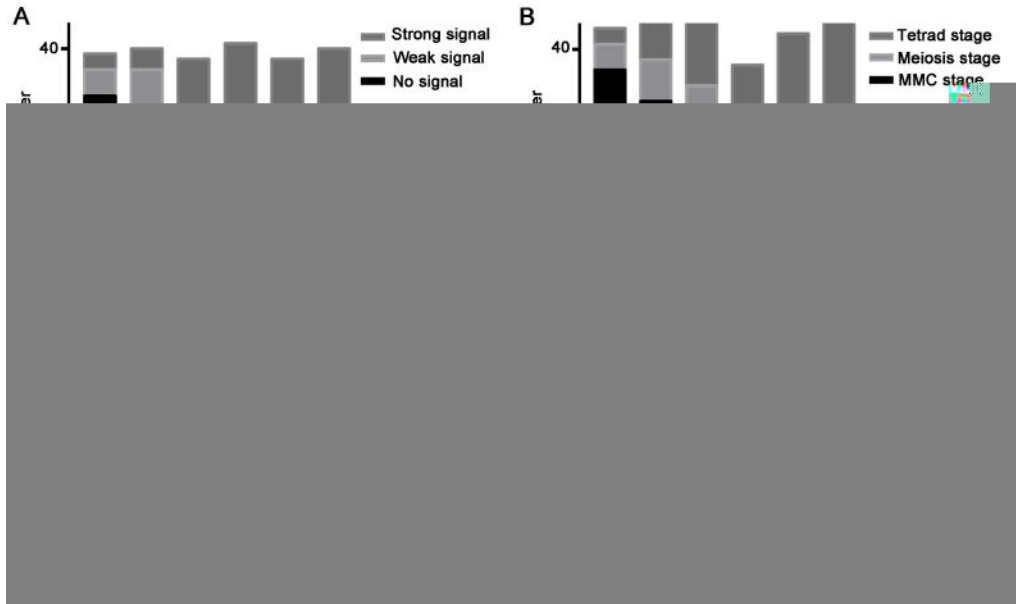(D) Ovule primordia height at stage 9a: 6 ovules per placenta (*n*=11).

(E) Ovule primordia height at stage 9b: 8 ovules per placenta (*n*=24).

(F) Ovule primordia height at stage 9c: 10 ovules per placenta (*n*=32).

(G) Proportions of parts of the placenta where the first ovule protrudes (*n*=187).

Differently colored lines highlight the representative placenta in (D–E).

Figure S2. Quantification of ovule number with different signals at different stages.

(A) Representative pistils at megaspore mother cell (MMC) differentiation stage, according to KUN-VENUS expression pattern (*n*=15).

(B) Representative pistil at the meiosis stage, according to KUN-VENUS expression pattern (*n*=15).

(C) Representative pistil at function magaspore (FM) differentiation stage, according *ProFM1::GUS* expression pattern *(n*=46).

(D) Representative pistil at the meiosis stage, according to CLSM observations (*n*=10).

Every column represents an independent pistil in (A–D).
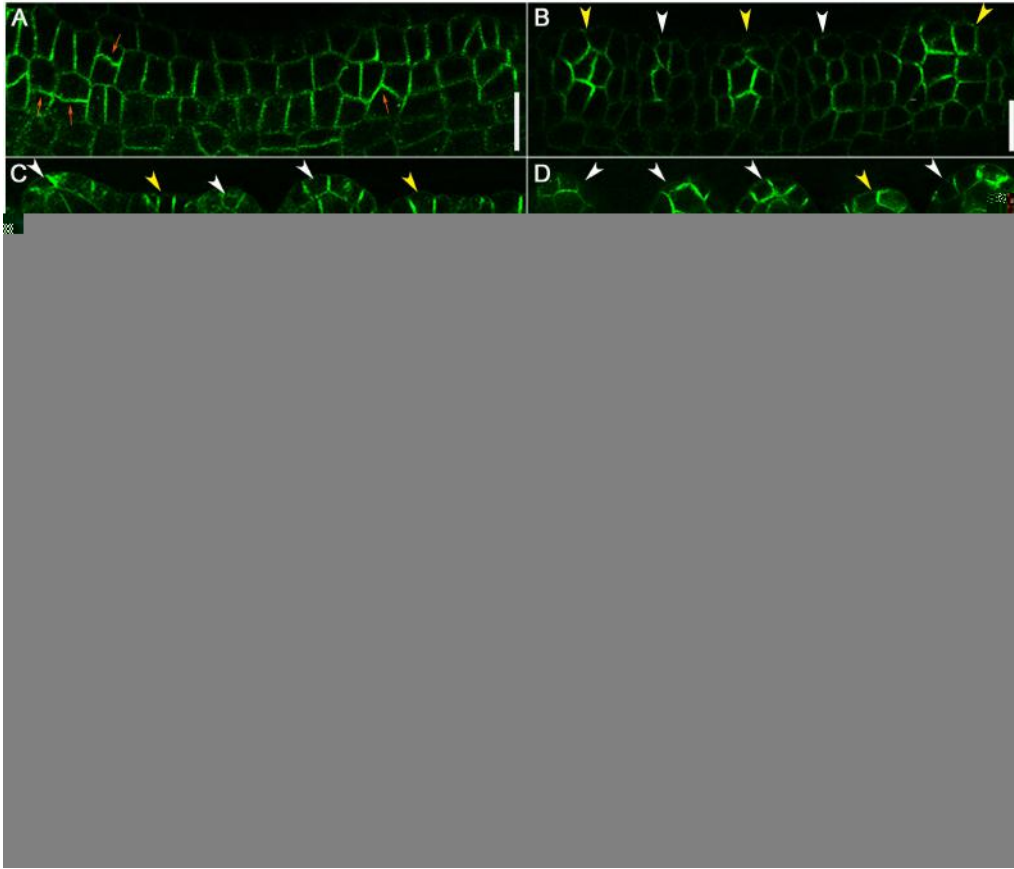
Figure S3. The distribution of *ProPIN::PIN-GFP* and *DR5::NLS-eGFP* in ovule primordia initiation process.

(A–D) *ProPIN1::PIN1-GFP* distribution in placentae at stage 8 (A), stage 9a (B), stage 9b (C), and stage 9c (D). Orange arrows point the cells in which the division direction changing, yellow arrowheads mark the young ovule primordia, white arrowheads mark the old ovule primordia (B–D).

(E–L) *DR5::NLS-eGFP* level and distribution. (E–H) *DR5::NLS-eGFP* merged with calcofluor white (cyan) stained cell wall. Dotted lines highlight the placenta in (E and I) and initiated ovule primordia in (F–H) and (J–L).

Bars = 20 μm in (A–D), 5 μm in (E–L).
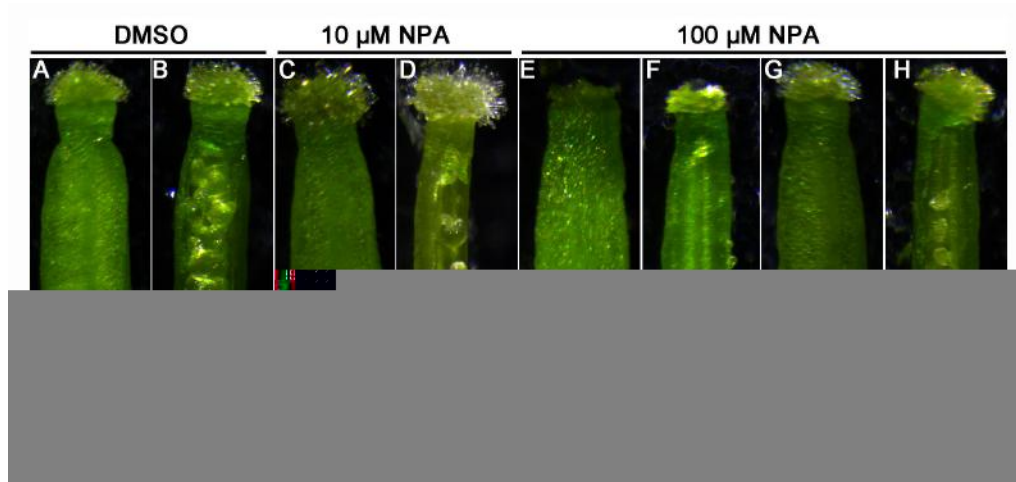
**Figure S4. NPA treatment in different concentrations.**

(A–B) The gynoecium (A) and ovules (B) at flower developmental stage 12 under DMSO treatment.

(C–D) The gynoecium (C) and ovule (D) at flower developmental stage 12 under 10 μM NPA treatment.

(E–H) The gynoecium (E, G), placenta (no ovule) (F), and ovule (H) at flower developmental stage 12 under 100 μM NPA treatment.

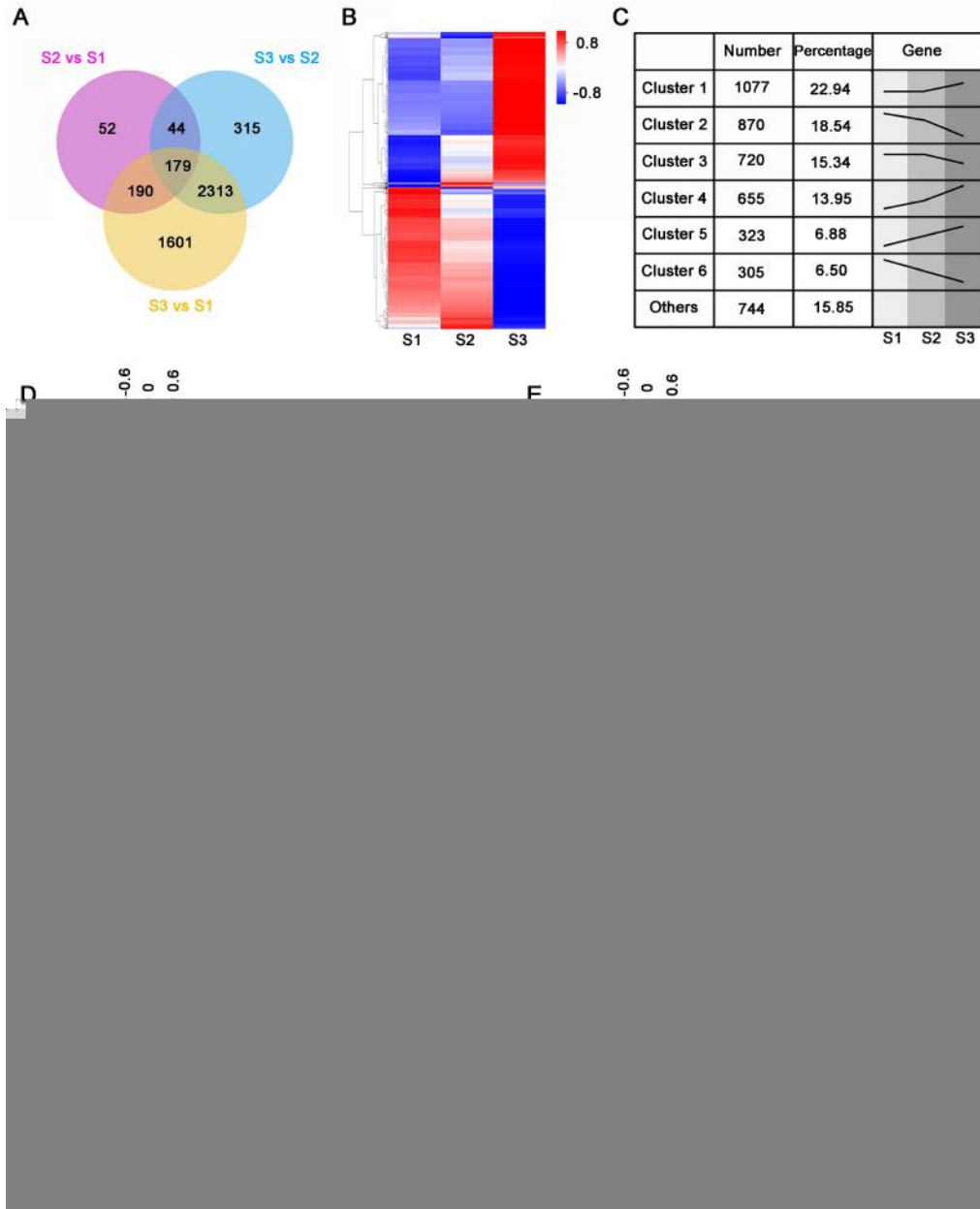The gynoecium was harvested for observation at 7 days after treatment.

Bar = 100 μm.
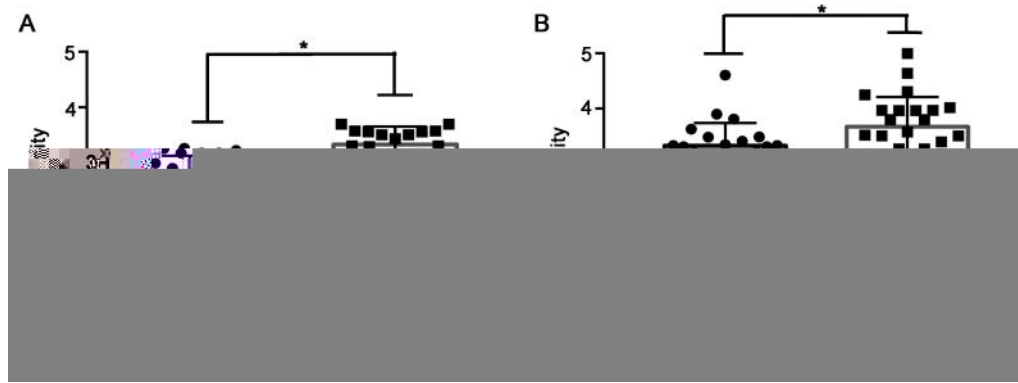
Figure S5. Ovule density in *bzr1-1D*.

(A) Ovule density at stage 9a, ovule density means the ratio of the ovule number to the placenta length per 100 μm.

(B) Ovule density at stage 9c.

The data are mean ± s.d.; n>15 in every group (one-way ANOVA; *P-value* < 0.05).

Figure S6. Microarray Analysis of the differentially expressed genes (DEGs) in ovule development at stage 9–10 (S1), stage 11 (S2), and stage 12 (S3).

(A) The number of DEGs between S1, S2, and S3.

(B) Heatmap of DEGs in S1, S2, and S3. The scale bar indicates the normalized signal value.

(C) These DEGs are clustered into main six clusters (1–6) based on their expression patterns in (B).

(D–G) Heat map visualizes the expression patterns of DEGs in the auxin signaling pathway (D), brassinosteroid signaling pathway (E), cytokinin signaling pathway (F), gibberellin signaling pathway (G). The scale bar indicates the normalized signal value.
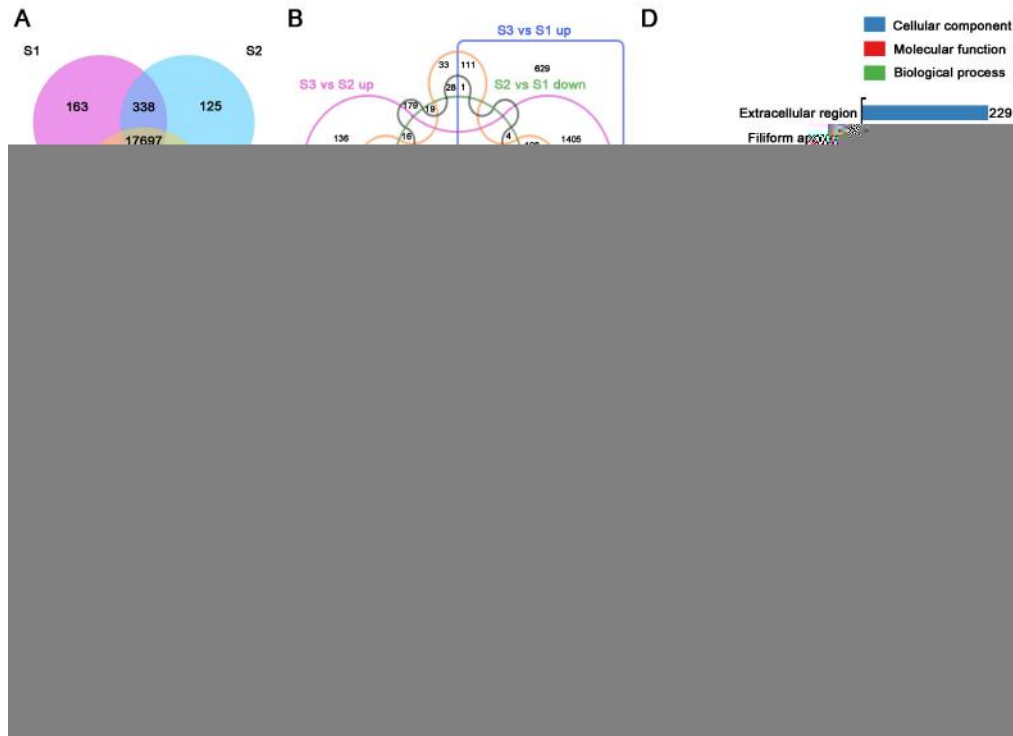
Figure S7. Overview of the detected genes and transcriptomic analysis of DEGs of pistils at stage 9–12.

(A) All genes we detected in stage 9–10 (S1), stage 11 (S2), stage 12 (S3).

(B) Overview of DEGs (upregulated and downregulated) between S1, S2, and S3.

(C) KEGG analysis shows that diverse pathways are enriched among the DEGs between S1, S2, and S3.

(D) Gene Ontology analysis of the DEGs between S1, S2, and S3. The numbers next to the column indicate the gene number.
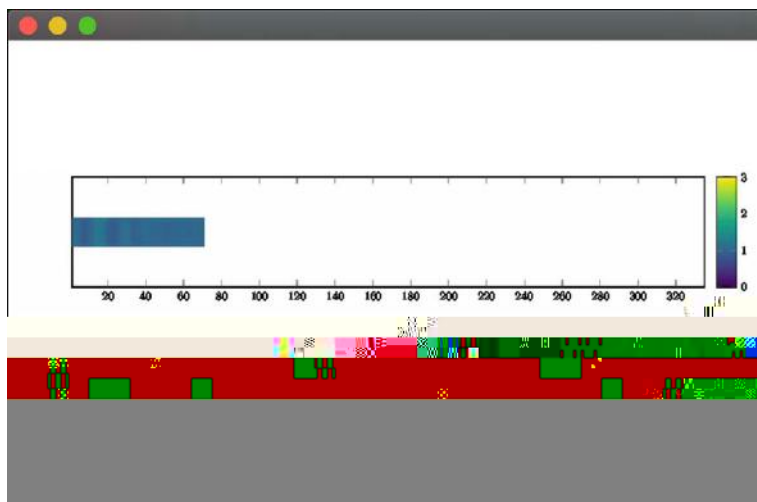
Table S1. List of Differentially Expressed Genes in S1-S3.

Click here to Download Table S1

Table S2. Genes involved in auxin, brassinosteroid, cytokinin, and gibberellin signaling among the DEGs.

Click here to Download Table S2

Movie 1. A computational model for auxin-regulated ovule initiation